Contributions of fine-particle magnetism to reading the global paleoclimate record (invited)

Subir K. Banerjee

Citation: Journal of Applied Physics **75**, 5925 (1994); doi: 10.1063/1.355517
View online: http://dx.doi.org/10.1063/1.355517
View Table of Contents: http://scitation.aip.org/content/aip/journal/jap/75/10?ver=pdfcov
Published by the AIP Publishing

Contributions of fine-particle magnetism to reading the global paleoclimate record (invited)

Subir K. Banerjee
Institute for Rock Magnetism, Department of Geology and Geophysics, University of Minnesota, 310 Pillsbury Drive, S.E., Minneapolis, Minnesota 55455

Paleoclimate changes are recorded by proxy as variations in concentration, composition, and grain size of magnetic minerals, principally magnetite (Fe_3O_4), in the sediments deposited in lakes, oceans, and continental eolian deposits. Cross-validated multiple-parameter magnetic measurements of such sediment cores provide global change data of high temporal resolution, useful for constructing a base-line record against which anthropogenic modifications may be discerned. Theories of superparamagnetism and magnetic domains are used to explain the physical basis of magnetic proxy recording. Examples of applications to validation of Milankovitch theory of climate change and delineation of the glacial and interglacial stages of the last 1 000 000 years are provided.

I. INTRODUCTION

Current interest in the possibility of rapid climate changes in the future triggered by anthropogenic alterations in the global climate system has led geologists and geophysicists to delineate very long-term (1000–100 000 years) paleoclimate changes for establishing base-line records. Geological records of decadal to century-scale climate changes are "written" in long ice cores from the polar regions, rapidly deposited sediments from certain lakes, and offshore marine sediments, as well as in windblown (eolian) dust deposits on continental sites. Such records are usually "read" by determining changes in (a) elemental and isotopic chemistry of ice and sediment grains, (b) size, shape, and amount of eolian grains, and (c) the type and character of trapped pollen grains representing the different vegetations of the past. Careful synthesis of these multiple proxy records of climate change can yield paleorecords of humidity, temperature, wind direction, and wind intensity. Some of the above proxy records can and do provide quantitative data, but all of them consume a lot of time for data gathering. Compared to this, magnetic proxies of climate change, a newcomer to the field, can only be classified currently as semiquantitative or qualitative, and yet the magnetic methods are becoming increasingly popular because of their high speed and sensitivity.

Researchers in rock magnetism use all the instruments that are commonly used in fine particle magnetism research plus some others that are particularly useful for measuring the weak remanent magnetizations (RM) that remain in a sample after application of a steady (or dc) magnetic field, or an alternating magnetic field (af) or variable temperatures, either singly or in combinations thereof. For comprehensive discussions of remanent magnetizations we refer the reader to some recent publications.[1–3] Fuller[4] has recently reviewed rock magnetic instrumentation. When combined with steady fields on the order of 50–100 μT, the same af demagnetizer can impart anhysteretic remanent magnetizations (ARMs) to samples. Partial ARMs (PARMs) are given by activating the steady field for given af windows, and hence only to certain selected grain sizes in an ensemble.[5]

II. POPULAR ROCK MAGNETIC PARAMETERS FOR SAMPLE CHARACTERIZATION

In addition to a strong preference for studying RMs, the other special characteristic of rock magnetism is the need to study whole samples without always subjecting them to magnetic separation, since magnetic separation preferentially extracts the high-susceptibility (χ) grains that may or may not be the same as the high-coercivity (H_c) grains that give rise to lab-imparted or natural RMs. A large effort has, therefore, gone into the development of instruments and techniques that are sensitive enough for characterizing weakly magnetic whole sediments or rocks. Second, whether the intended application is to decipher climate change proxies or to determine the source of sediments in a stream, the rock magnetic parameters are chosen for their sensitivity to changes in concentration, composition, and grain size. For example, as humidity and temperature change from one climate regime to the other, the magnetic minerals undergo chemical and/or microstructural changes. We need to first recognize these subtle changes in the presence of a vast paramagnetic "noise," and then interpret them in terms of paleoenvironmental "signal."

A. Concentration-dependent parameters

Strongly magnetic (93 A m^2/kg) magnetite is usually the dominant magnetic mineral whose relative concentration (with depth, say) can be determined by measuring the variations in saturation magnetization J_s or low-field susceptibility χ, if the grains are only large multidomain (MD), say, above 10 μm and if no depth-dependent chemical change is present. If magnetite content falls below ten parts per million, as in organic-rich peat, saturation isothermal remanence (SIRM or J_{rs}) serves as a sensitive concentration-dependent

 0021-8979/94/75(10)/5925/6/$6.00

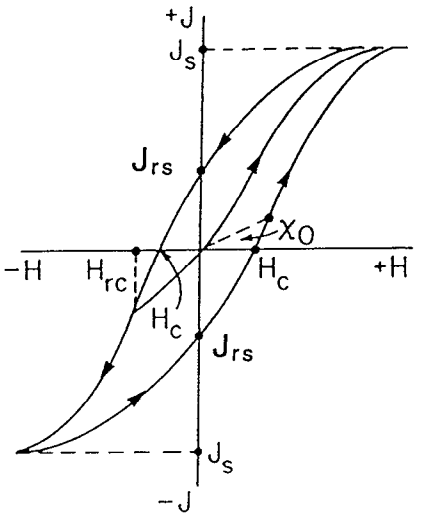

FIG. 1. A major (high-field) hysteresis loop (Ref. 1), showing saturation magnetization J_s, saturation isothermal remanent magnetization J_{rs}, coercivity of remanence H_{cr}, coercive force H_c, and low-field susceptibility χ_0.

parameter since the magnetite-free part of peat is paramagnetic or diamagnetic, unable to acquire remanence.

B. Composition-dependent parameters

The most intrinsic composition-dependent parameter is the Curie point, but it is frequently necessary to ascertain it from a mostly paramagnetic sample with a small (<0.1%) ferrimagnetic content, resulting in poor precision. Also, titanium (Ti^{4+}) ions can occur as a substitution for iron ions and lower the Curie point. Although calibration curves for titanium substitution are available,[1] in a totally "blind" situation a Curie point of 623 K could well signify the presence of pyrrhotite ($Fe_{(1-x)}S$), a titanomagnetite ($Fe_{2.6}Ti_{0.4}O_4$), a titanohematite ($Fe_{2.4}Ti_{0.6}O_3$), or a slightly cation-deficient titonomagnetite with appropriate titanium substitution.

X-ray diffraction or selected-area electron diffraction of the magnetic extract is usually attempted to confirm the composition; but, this too fails often due to low concentration or ultrafine grain size of the magnetic fraction. In such cases, Curie point data are combined with other composition-sensitive parameters, especially temperature dependence of magnetocrystalline anisotropy constant K or stepwise demagnetization of J_{rs} to determine H_{cr} (Fig. 1), the remanence coercivity, which is very different for magnetite and hematite.

Pyrrhotite, magnetite, and hematite all have characteristic temperatures for spin reorientation reflecting a change in sign of K.[1] Saturation isothermal remanent magnetization J_{rs} is given to pyrrhotite and magnetite at, say, 4.2 K in a field of 1.5 T and then the sample is warmed in the field-free space of a susceptometer to discover sharp drops in J_{rs} at the characteristic transition temperatures T_t, which are 34 and 120 K respectively, for pyrrhotite and magnetite. Hematite displays a T_t when room temperature J_{rs} is cooled to 263 K.

For distinguishing magnetite from hematite at 300 K, the parameters S and HIRM (given below) have been defined[6,7] which take advantage of their large difference in H_{cr} (see Fig. 1 for H_{cr}),

$$S=-(\mathrm{IRM}_{-300\ \mathrm{mT}})/J_{rs},$$

$$\mathrm{HIRM}=(J_{rs}+\mathrm{IRM}_{-300\ \mathrm{mT}})/2.$$

The symbol $\mathrm{IRM}_{-300\ \mathrm{mT}}$ signifies the RM obtained by first saturating the sample in +1.5 T, and then applying −300 mT to demagnetize the magnetite component of J_{rs}. The remaining RM is due to the higher-coercivity hematite fraction, because while magnetite saturates at 300 mT, hematite requires 1000 mT or more. In the absence of hematite, $S\cong 1$ whereas in the absence of magnetite HIRM≅1.

C. Grain-size-dependent parameters

Although magnetic properties are not directly related to actual grain size, they do reflect the presence or absence of (i) magnetic relaxation phenomena and (ii) magnetic domains and their relative number in a sample. We list below the most popular parameters measured at room temperature by rock magnetists to find out where the mean or median value of a given size distribution occurs with respect to three critical size thresholds for magnetic transitions: (i) superparamagnetic (SP) to thermally stable d_s; (ii) single-domain (SD) to two-domain d_0; and (iii) pseudosingle-domain (PSD) to "true multidomain" (MD) transition d_m. Table I lists the threshold values for cubic magnetite determined by different authors either experimentally, or from theory of (i) *a priori* equilibrium domain states, or (ii) the more general nonequilibrium micromagnetic models.[2,15]

The notation d_{max} refers to the theoretical maximum size possible for SD state when the grain is only in a local energy minimum. For those interested in remanent magnetization, the pseudosingle-domain (PSD) range[16,17] of magnetite, 0.08 to ~10 μm, is a very useful empirical size window. PSD grains have RM values less than SD but their stability to af demagnetization and H_{cr} values is high like SD grains.

The critical volume V_B above which superparamagnetism (i.e., high χ but no RM) disappears was given by Bean and Livingston[18] as:

$$V_B=2kT\ \ln(f_0 t)/\mu_0 M_s H_k,$$

where k is Boltzmann's constant, attempt frequency $f_0=1\times10^{-9}\ \mathrm{s}^{-1}$, t is measuring time, μ_0 is the free air permeability, M_s is saturation magnetization, and H_k is the microscopic coercive force. Lowering temperature T or mea-

TABLE I. Threshold values for cubic magnetite determined by different authors.

d_s (μm)	d_0 (μm)	d_{max} (μm)	d_m (μm)
0.03 (expt.)[a]	0.05 (expt.)[a]	0.28 (all theor.)[f]	
0.025 (expt.)[b]	0.08 (theor.)[c]	0.11[g]	8.0 (theor.)
	0.12 (theor.)[a]	0.24[e]	
	0.10 (theor.)[e]	0.14[h]	

[a]From Ref. 8.
[b]From Ref. 9.
[c]From Refs. 10–12.
[d]From Ref. 13.
[e]From Ref. 14.
[f]From Ref. 11.
[g]From Ref. 12.
[h]From Ref. 15.

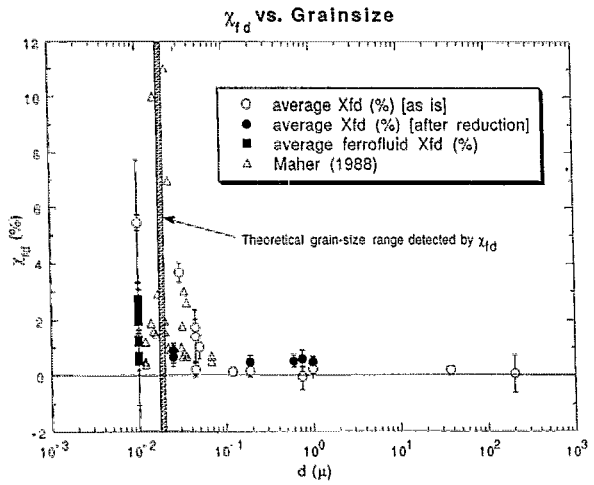

FIG. 2. Percentage change in χ when measured at 500 and 5000 Hz. It can only detect magnetite grains between 18 and 20 nm. Hollow circles denote cation-deficient magnetite.

surement time t leads to thermally stable SD behavior when RM becomes stable and low-field susceptibility χ is small. Therefore, a common technique at 300 K for detecting SP grains has been to measure the percentage decrease χ_{fd} in χ when measured at about 500 and 5000 Hz.[19] Thus, $\chi_{fd}=100(\chi_{500}-\chi_{5000})/\chi_{500}$. It has been pointed out[20] that according to Néel's theory of magnetic relaxation χ_{fd} above reflects grains between 18 and 20 nm only, not all the SP grains at 300 K for magnetite, 0–30 nm. Hunt, Kletetschka, and Sun[21] have now shown (Fig. 2) that experimental data on χ_{fd} of synthetic magnetite confirms the above statement and a different approach (Fig. 6 below) is necessary to determine the complete SP fraction in a sample.

Next, we discuss the detection of grains larger than SP, i.e., SD, PSD, and MD. The most frequently used method[22] for relative grain-size determination for thermally stable grains is to plot hysteresis parameters J_{rs}/J_s vs H_{cr}/H_c [Fig. 3(a)], after cycling a magnetite-bearing sample in a large saturating field, say, 500 mT. Uniaxial single-domain grains, in the absence of grain interactions, should display $J_{rs}/J_s=0.5$ and $H_{cr}/H_c=1.5$, while the largest or "true" multidomain samples have J_{rs}/J_s values <0.10 and $H_{cr}/H_c>3.5$. As seen in Fig. 3(a), there is no sharp transition in the magnetic parameters above the classical single-domain–to–two-domain threshold d_0. Instead, there is a smooth transition spanning the pseudosingle-domain region, 0.1–10 μm. A major deficiency of Fig. 3(a) is that it cannot distinguish between (i) a mixture of sizes, say, 0.5 and 40 μm, and (ii) a homogeneous sample of 10 μm. Jackson, Worm, and Banerjee[23] find that Fourier analysis of the hysteresis loop can, however, accomplish that goal.

Figure 3(b) shows that ARM intensity J_{ar} vs χ data for magnetite[24] are useful for distinguishing grainsizes below 20 μm, which is the threshold for easy observation in an optical microscope. The slope J_{ar}/χ increases rapidly between 1.0 and 0.1 μm (near the SD threshold), and the apparent slight increase in χ is an artifact of unavoidable admixtures of SP grains in the experimental samples of small median size. Experimental data of J_{rs} and H_{cr} have also been used by Thompson and Oldfield[7] to construct Fig. 4, to identify the different magnetic domain states of magnetite, as well as to indicate the presence of hematite in a given mixture through its unusually high coercivity of remanence ($H_{cr}>200$–300 μT).

III. MAGNETIC RECORDS OF PAST CLIMATE CHANGE

The most reliable magnetic proxies of climate change have come from concentration variation of magnetite in ma-

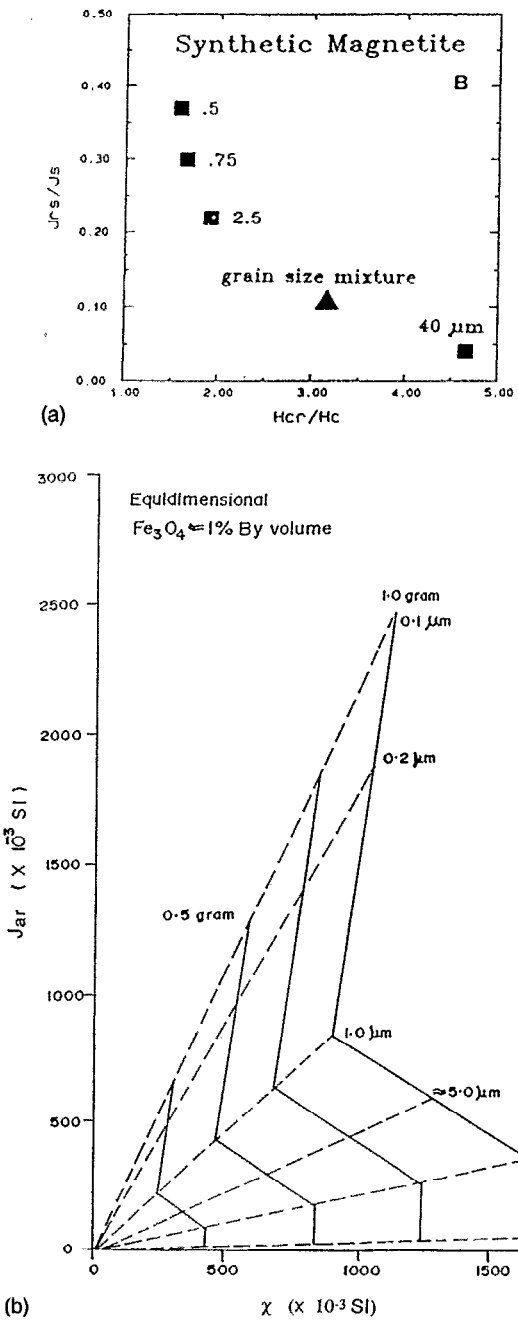

FIG. 3. (a) Jackson and co-workers' demonstration (Ref. 23) that mixtures of 0.5 and 40 mm grain appear like ~10 μm if characterized by J_{rs}/J_s vs H_{cr}/H_c plots. (b) King *et al.*'s calibration curve (Ref. 24) for magnetite granulometry using ARM intensity, J_{ar}, and χ parameters. High slope denotes finer grain size.

rine sediments. Such magnetite owes its origin[7] to (i) distant volcanic eruptions and forest fires, or (ii) ice-rafted detritus during warm interglacial times, or (iii) monsoon winds blowing over arid land. Prior to our discovery of the magnetic proxies, much effort was spent in testing geologically the so-called Milankovitch theory of ice ages. This theory claims that variations in the (i) eccentricity of the Earth's orbit around the Sun, (ii) the obliquity or tilt of the Earth's rotation axis, and (iii) the precessional motion of the Earth's poles—all three contribute to variations in insolation from the Sun, and cause periodic cold glacial and warm interglacial times.[25] We discuss here three situations where the availability of high-precision and high-resolution magnetic susceptibility data have confirmed many details of the Milankovitch theory.

First, Blomendahl *et al.* have studied χ versus depth obtained from four widely separated cores of ocean sediments in the eastern Atlantic, next to west Africa.[26] They have shown that χ profiles correlate very well with variations in the glacial ice sheets that carry magnetite-bearing rock debris to lower latitudes during warmer times. Second, they have observed similar records of changes in wind-borne magnetite

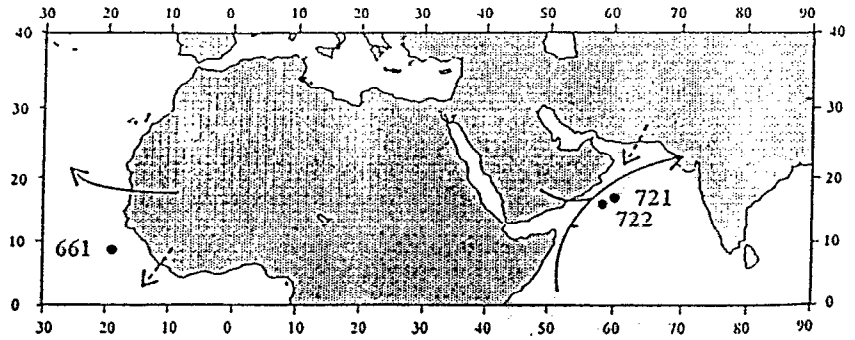

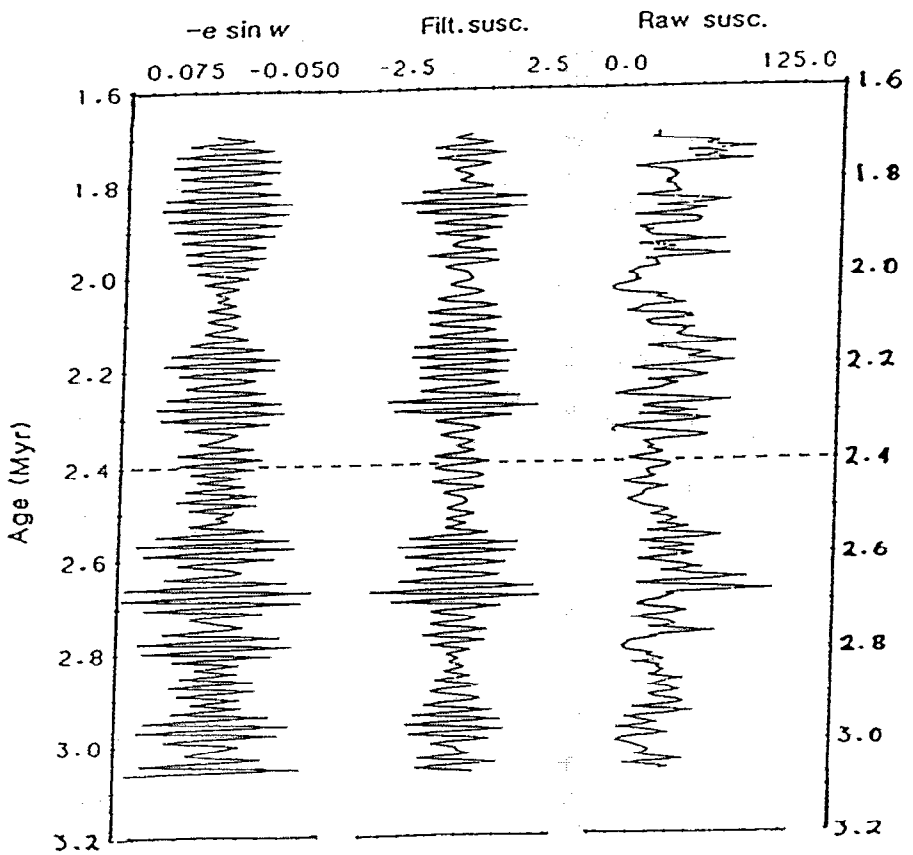

FIG. 4. Kukla *et al.*'s demonstration (Ref. 28) that oceanic temperatures (glacial/interglacial) from $\delta^{18}O$ data are reflected in the χ logs from two sites in central China. The arrows at the bottom of all profiles represent 730 000 years. Glacial/interglacial stages (even/odd) shown on the right-hand side.

in the Arabian sea as a proxy of changes in the intensity of paleomonsoons off the Arabian coast.[27]

Finally, we owe to magnetism our first attempts at a high-resolution comparison of oceanic and continental climates. Most of the reliable proxy data for global climate change over the last 1 000 000 years have come from the variations in oxygen isotopes ($\delta^{18}O$, which measures departures from a standard ratio of $^{18}O/^{16}O$) preserved in the $CaCO_3$ shells of fossil foraminifera in ocean sediments. Such globally averaged (or SPECMAP) $\delta^{18}O$ on the right-hand side of Fig. 4 was shown by Kukla *et al.*[28] to compare well in character with the χ versus depth data from Xifeng and Luochuan in the central Chinese loess plateau. It was claimed that during glacial times, strong winds from the desert bring nonmagnetic silicates which dilute the concentration of the worldwide "rain" of magnetite caused by volcanic eruptions and forest fires. Hence, Kukla *et al.* concluded that low temperatures in central China (low χ) have varied in phase with low temperatures recorded by the ocean sediments (high $\delta^{18}O$).

Hovan *et al.*[29] have now shown that the $\delta^{18}O$ record from a sediment core in the northwest Pacific follows the accepted globally averaged (SPECMAP) ice volume record. They then show that the eolian flux of separated sand grains in their core show signs of strong aridity and high wind speed (i.e., greater flux) during the colder glacial times (positive $\delta^{18}O$ values).

However, their correlations are only approximate, because when the Xifeng magnetic record is independently dated by the presence of a known geomagnetic polarity reversal, it does not match exactly the eolian flux record. Thus, the locations of interglacial S layers had to be "corrected" downward in order to match the oceanic climate record in eolian flux. I now believe that the lack of an exact fit is due to an incorrect model for χ variation, but this attempt by Hovan *et al.* was an important first step toward establishing a direct correlation between continental and oceanic climate records.

Maher and Thompson's work[30] shows that the problem above owes its origin, at least partly, to two sources of magnetite in the high susceptibility S layers. One source is indeed magnetite brought from elsewhere. The other is fine-grained superparamagnetic (SP) magnetite produced *in situ* by pedogenic alteration (soil forming) of paramagnetic silicate due to high humidity and temperature during summer monsoons. The magnetic proxy record thus contains both the global climate record and its regional modification. We have now developed a method[20] to estimate the total SP fraction from each horizon and contrasted this fraction for two nearby sites in China, Baicaoyuan and Xifeng, separated by Liupanshaan, a mountain range which causes a rain shadow in the arid site, Baicaoyuan.

Our method depends on warming a high-field (2.5 T) low-temperature (15 K) J_{rs} in zero field to separate the temperature-dependent loss of remanence by all grains that are SP at 300 K from the remanence carried by coarse-grained magnetite, distinguished by their sharp Verwey transition at ~120 K. Figure 5 shows the comparison of a glacial loess (L_{1a}) and its overlying interglacial soil (S_o) with a synthetic mixture of 50:50 SP and MD magnetite. Graphical methods of extrapolation of SP remanence to 15 K allow the estimation of the SP contribution which is then divided by the total J_{rs} at 15 K to obtain SP/total fractions shown in Fig. 6(a). This fraction, and not low-field χ, more accurately represents past changes in summer monsoon intensity.

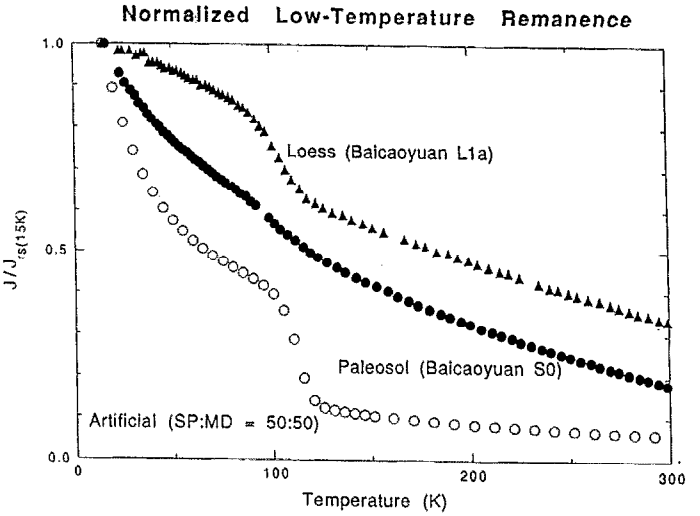

FIG. 5. Warming of 2.5 T J_{rs} (15 K) in zero field shows different characters for loess (less SP grains) and overlying soil (more SP) from Baicaoyuan. The temperature-dependent SP remanence is extrapolated to 15 K to obtain relative fraction, SP/total.

Our data show that during the coldest glacial periods, L_2 and L_{1c}, both sites show the expected minima in SP fraction; but, the more humid site, Xifeng, has a consistently higher fraction of SP grains due to greater local pedogenesis. The difference between the two profiles (arid Baicaoyuan, humid Xifeng) thus allows us to observe the regional variations in the impact of global climate changes. Even an unexpected observation, that during S_o time (5–10 ka before present) both sites had similar pedogenesis has been confirmed independently. Figure 6(b) shows the bulk grain-size variation of whole sediments (magnetic and non-magnetic) of the S_o horizons of the two sites. Both the magnetic and bulk grain-size data say that pedogenesis was the same during S_o time. One possible interpretation is that at this time the summer monsoon came from South China Sea, parallel to the mountain range, thus removing the rain shadow. Future detailed work at these and other sites in the Chinese loess plateau are ongoing, both at our laboratory and elsewhere. The goal is to separate true global climate change signatures from the regional ones for Asia, so that we can finally attempt a valid comparison between global oceanic and continental climates and verify the validity of the current numerical paleoclimate models for predicting past temperatures for the whole Earth.

ACKNOWLEDGMENTS

This study was supported by NSF Grant No. EAR 9206024. The Institute for Rock Magnetism is funded by the Keck Foundation, the National Science Foundation, and the University of Minnesota. I thank Diana Jensen and Michelle

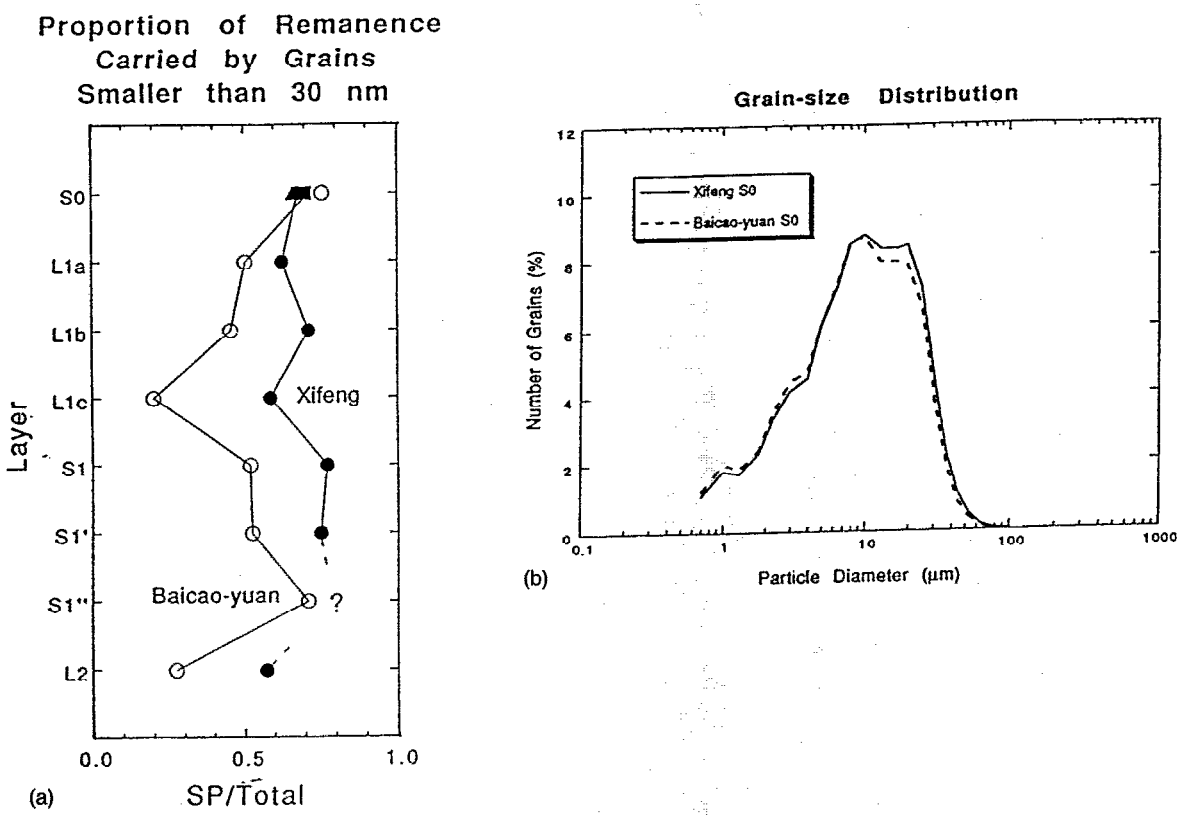

FIG. 6. (a) Left-hand side: variation of SP/total, i.e., summer monsoon intensity between arid Baicaoyuan and humid Xifeng (Ref. 20). The high rainfall at Xifeng produces high SP content. The difference between the two provides regional climate information. (b) Right-hand side: during formation of layer S_0 (5000–10 000 years ago) both sites enjoyed similar humidity to produce a similar amount of coarse and fine grains, as shown in the bulk grain-size variation. It would be possible if the summer monsoon was then from the south, rather than east.

Elston for help in preparing the manuscript. This is publication no. 9310 of the Institute for Rock Magnetism.

[1] C. P. Hunt, B. M. Moskowitz, and S. K. Banerjee, in *Handbook of Physical Constants*, edited by T. Ahrens (American Geophysical Union, Washington, D.C., in press).
[2] D. J. Dunlop, Rep. Prog. Phys. **53**, 707 (1990).
[3] S. K. Banerjee, in *Geomagnetism*, edited by J. A. Jacobs (Academic, San Diego, 1989), Vol. 3, p. 1.
[4] M. D. Fuller, in *Methods of Experimental Physics*, 24A edited by C. G. Sammis and T. L. Henyey (Academic, Orlando, 1987), Vol. 24A, p. 303.
[5] M. J. Jackson, W. Gruber, J. Marvin, and S. K. Banerjee, Geophys. Res. Lett. **15**, 440 (1988).
[6] R. Thompson and F. Oldfield, *Environmental Magnetism* (Allen and Unwin, London, 1986), p. 229.
[7] J. W. King and J. E. T. Channell, Rev. Geophys. **29**, Suppl, 358 (1991).
[8] D. J. Dunlop, J. Geophys. Res. **78**, 1780 (1973).
[9] D. J. Dunlop and M.-M. Bina, Geophys. J. R. Astron. Soc. **51**, 121 (1977).
[10] B. M. Moskowitz and S. K. Banerjee, IEEE Trans. Magn. **MAG-15**, 1241 (1979).
[11] T. S. Moon and R. T. Merrill, Phys. Earth Planet. Inter. **37**, 214 (1985).
[12] R. J. Enkin and D. J. Dunlop, J. Geophys. Res. **92**, 12726 (1987).
[13] F. Heider and W. Williams, Geophys. Res. Lett. **15**, 184 (1988).
[14] W. Williams and D. J. Dunlop, Nature **337**, 634 (1989).
[15] V. P. Shcherbakov and B. E. Lamash, Geophys. Res. Lett. **15**, 526 (1988).
[16] S. K. Banerjee, J. Geomagn. Geoelectr. **29**, 319 (1977).
[17] D. J. Dunlop, J. Geomagn. Geoelectr. **29**, 293 (1977).
[18] C. P. Bean and J. D. Livingston, J. Appl. Phys. **30**, 120 (1959).
[19] F. Heller, X. M. Liu, T. S. Liu, and T. C. Xu, Earth Planet. Sci. Lett. **103**, 301 (1991).
[20] S. K. Banerjee, C. P. Hunt, and X. M. Liu, Geophys. Res. Lett. **20**, 843 (1993).
[21] C. P. Hunt, G. Kletetschka, and W. W. Sun (unpublished).
[22] R. Day, J. Geomagn. Geoelectr. **29**, 233 (1977).
[23] M. J. Jackson, H. U. Worm, and S. K. Banerjee, Phys. Earth Planet. Inter. **65**, 78 (1990).
[24] J. King, S. K. Banerjee, J. Marvin, and Ö. Özdemir, Earth Planet. Sci. Lett. **59**, 404 (1982).
[25] J. Imbrie, in *Milankovitch and Climate: Understanding the response to Orbital forcing, Part I*, edited by A. Berger, J. Imbrie, J. Hays, G. Kukla, and B. Saltzman (Reidel, Dordrecht, 1984), p. 269.
[26] J. Blomendal, B. Lamb, and J. King, Paleoceanography **3**, 61 (1988).
[27] J. Blomendal and P. deMenocal, Nature **342**, 897 (1989).
[28] G. Kukla, F. Heller, X. M. Liu, T. C. Xu, T. S. Liu, and Z. S. An, Geology **16**, 811 (1988).
[29] S. A. Hovan, D. K. Rea, N. G. Pisias, and N. J. Shackleton, Nature **340**, 296 (1989).
[30] B. A. Maher and R. Thompson, Geology **19**, 3 (1991).